European Review for Medical and Pharmacological Sciences 2021; 25: 866-879

Effect of TLR7 gene expression mediating NF-κB signaling pathway on the pathogenesis of bronchial asthma in mice and the intervention role of IFN-γ

L. SONG, B. LUAN, Q.-R. XU, X.-F. WANG

Department of Pediatric Respiratory Medicine, the Third Affiliated Hospital of Zhengzhou University, Zhengzhou City, Henan Province, P.R. China

Abstract. – OBJECTIVE: To explore the mechanism of TLR7 mediating NF-κB signaling pathway on the pathogenesis of bronchial asthma in mice and the intervention effect of IFN-γ in the process.

MATERIALS AND METHODS: The experimental animals were 70 C57BL/6J female mice of clean grade, which were divided into 7 groups according to different treatment protocols, including Normal group, Asthma group, Model+1-MT group, Model+IFN-γ group, Model+TLR7 agonist group, TLR7 deficient group, and Model+TLR7 deficient group. Hematoxylin-eosin (HE) staining was used to observe the pathological changes of lung tissues. The positive expression rates of TLR7, p-IKKα and NF-κBp65 were detected by immunohistochemistry. bronchoalveolar lavage fluid (BALF) cells were classified and counted. The contents of interleukin (IL)-4, IL-10, IL-12 and interferon (IFN)-γ in BALF supernatant were detected by enzyme-linked immunosorbent assay (ELISA). Following isolation, culture and plasmid construction of airway smooth muscle cells (ASMCS) from normal mice and asthmatic mice, cells were transfected and divided into the Control group, pcDNA-TLR7 NC group, siRNA-TLR7 NC group, pcDNA-TLR7 group, siRNA-TLR7 group, Asatone group, Triptolide group, and pcDNA-TLR7 +Asatone group. The expression of TLR7, IDO, p-IKKα and NF-κBp65 was detected by real-time polymerase chain reaction (RT-PCR) and Western blot, respectively. 3-(4,5-dimethyl-2-thiazolyl)-2,5-diphenyl-2-H-tetrazolium bromide (MTT) was used to detect the proliferation of ASMCS. The cell cycle and apoptosis of ASMCS were detected by flow cytometry.

RESULTS: HE staining showed successful modeling of asthma. Immunohistochemical test showed that the positive expression rate of TLR7 in the Asthma group was significantly decreased, and that of IKKα and NF-κBp65 was significantly increased, with significantly increased IL-4, IL-10, IL-12 and IFN-γ levels (all $p<0.05$). Model+1-MT group and Model+TLR7 deficient group had a large number of inflammatory cell infiltration, increased IL-4, IL-10, IL-12 and IFN-γ levels, decreased expression levels of TLR7 and IDO, and increased expression of p-IKKα and NF-κBp65 (all $p<0.05$); while the opposites results were detected in Model+IFN-γ group and Model+TLR7 agonist group (all $p<0.05$). Cell transfection experiments revealed that pcDNA-TLR7 group and Triptolide group had increased TLR7 expression while decreased p-IKKα and NF-κBp65, decreased proliferation level, and increased cell apoptosis (all $p<0.05$); while the contrary results were found in siRNA-TLR7 group and Asatone group (all $p<0.05$); yet without significant difference in pcDNA-TLR7+Asatone group (all $p>0.05$).

CONCLUSIONS: Upregulation of TLR7 can inhibit the activation of NF-κB signaling pathway, reduces airway inflammation, inhibits ASMCS proliferation and thus promotes cell apoptosis in asthmatic mice. Besides, IFN-γ can exert a protective role in suppressing the progression of inflammation in asthma.

Key Words:

TLR7, NF-κB signaling pathway, Bronchial asthma, Airway inflammation, Airway smooth muscle cells, Proliferation, Apoptosis

Introduction

Immunologic tolerance is a kind of specific immune non-responsive state produced by the immune system after contacting with antigenic substances[1]. It plays a key role in the body's adaptation to the external environment (such as contact with external antigens) and non-responsive protection of its own tissue antigens[2]. The immunologic tolerance can be induced to

Corresponding Author: Bin Luan, MM; e-mail: luanbp117@163.com

prevent and treat diseases such as transplant rejection, autoimmune and allergic diseases[3,4]. Bronchial asthma is an allergic disorder featured by airway hyperresponsiveness and chronic airway inflammation[5]. Activation of naive CD4+ T cells is the initiating factor in the pathogenesis of asthma, and the imbalance of Th1/Th2 cells is considered to be a key link in its occurrence[6]. Insufficient apoptosis of activated T lymphocytes can be detected in patients with allergic asthma, which is an important reason for frequent occurrence and chronic delay of the disease and may be the evidence of the deficiency of immune tolerance mechanism in its pathogenesis[7]. The absence or weakening of immune tolerance can further enhance Th2 response, further induce airway hyperresponsiveness and thus result in chronic inflammatory diseases eventually[8,9]. Hence, the deficiency of immune tolerance mechanism may be the primary cause of allergic asthma.

Indoleamine dioxygenase (IDO) mediated tryptophan metabolism has been documented to play an important role in peripheral immune tolerance, and its role in allergic asthma, organ transplantation and tumor has become a research hotspot in recent years[10,11]. Expression of IDO at transcriptional level in various cells may be induced by specific inflammatory factors, and interferon (IFN)-γ is one of the typical factors which is the common inducer of IDO[12]. Other inflammatory factors such as IFN-α, IFN-β and LPS can also induce IDO expression, but the induction effect is not as good as that of IFN-γ[13]. Studies on the mechanism of IDO expression change induced by IFN-γ have detected that it may be regulated by many proinflammatory cytokines such as IL-1β, TNF-α, NF-κB, etc.[14]. Among them, NF-κB is composed of p65 subunit and p50 subunit and plays a pivotal role in inflammation and immune response by regulating cascade amplification cascade effect between immune/inflammatory related factors and inflammatory mediators[15,16]. The airway tissue reconstruction in asthma exhibits an intimate association with the activation of NF-κB, such as proliferation of airway epithelial cells, fibrosis of airway surrounding tissues, proliferation and hypertrophy of smooth muscle cells[17,18]. Moreover, the progression of asthma is closely related to the sustained and excessive expression of inflammatory factors caused by NF-κB activation[19]. These proinflammatory cytokines are regulated by downstream products of toll-like receptors (TLRs) signaling pathway, suggesting that IDO may be associated with TLRs[20]. In the research of establishing tumor microenvironment for effective immunotherapy, it has been shown that inhibition of IDO activity can further enhance the antitumor activity of TLR9 agonist IMO-2125[21]. In addition, IDO inhibitor 1-methyl-tryptophan (1-MT) can interfere with TLR signaling transduction in dendritic cells (DCs) independently of IDO activity[22]. However, the relationship between IDO and members in TLRs in allergic asthma is not clear so far.

As pattern recognition receptors, TLRs play a key role in the process of pathogen infection[23]. At present, 10 different TLRs (named from TLR1 to TLR10), have been found in human beings[24]. The role of TLRs in the development of asthma has been widely concerned. At present, it is believed that TLR4 expression is quite important for the activation of DCs in mice[25]. The activation of DCs leads to the upregulation of costimulatory molecules and the release of Th2 cytokines, which mediates the increase and exudation of eosinophils, thus leading to airway inflammation, suggesting that TLR4 activation is one of the causes of asthma[26]. Meanwhile, gene polymorphisms of other TLRs also affect the susceptibility and course of asthma[27,28]. TLR7 activation also plays an important role in the occurrence and development of allergic diseases and autoimmune diseases[29,30]. IFN-α, IL-12 and TNF-α produced after TLR7 activation can mediate the immune response to shift to the direction dominated by Th1 cells, correct the dominant role of Th2 cells in asthmatic patients, reduce the expression of IL-4 and IL-13, and thus achieve the purpose of relieving asthma symptoms[31]. In particular, in asthmatic animal model, mice treated with topical TLR7 agonist imiquimod (an immune modulator) showed decreased alveolar macrophages, B cells and TNF-α, and increased secretion of DCs, NK cells and IL-10 simultaneously, showing the therapeutic effect of asthma[32]. It supports that TLR7 has great potential in the treatment of allergic asthma.

In view of the above interpretation, and considering that there are few researches related to the role of TLR7 and NF-κB in the development of asthma, the present study was carried out to investigate the mechanism of TLR7 mediating NF-κB signaling pathway on the pathogenesis of bronchial asthma in mice and reveal the intervention effect of IFN-γ.

Materials and Methods

Modeling and Grouping

The experimental animals were 70 C57BL/6J female mice of clean grade, weighing 13-18 g and 7 weeks old, which were purchased from the Experimental Animal Center of Nanjing Medical University. Used animals were divided into 7 groups according to different treatment protocols: Normal group, Asthma group, Model+1-MT group (1-MT, IDO inhibitor, increase the inflammatory reaction), Model+IFN-γ group (IFN-γ, IDO inducer, suppress the inflammatory reaction), Model+TLR7 agonist group, TLR7 deficient group, and Model+TLR7 deficient group, with 10 mice in each group. As for the construction method of each group, it was described as follows: (1) mice in normal group did not receive any modeling treatment but just gastric administration of sterile distilled water. (2) Asthma group: a mouse model of asthma induced by dust mite was established by intraperitoneal injection of dust mite antigen extract and aluminum hydroxide (20 μg/2 mg) combined with nasal challenge with dust mite antigen at a concentration of 4 mg/mL. The successful modeling mice could show typical symptoms of asthma attack, such as rapid breathing, erect hair, cyanosis of lips, forelimb retraction, limb paralysis, slow response, nodding respiration and other symptoms. Two mice with asthma symptoms were randomly selected and lung tissue sections were collected for observation to verify the successful modeling. (3) Model+1-MT group: after successful establishment modeling as that of the Model group, mice were given 1-MT of IDO inhibitor (0.2 ml/kg for each) at the concentration of 2 mg/ml for one week of abdominal injection. (4) Model+IFN-γ group: Modeling mice in this group were given 100 U/ml IDO inducer IFN-γ for one week of continuous atomization. (5) Model+TLR7 agonist group: Modeling mice in this group were provided with TLR7 agonist by gavage for one week continuously. (6) TLR7 deficient group: TLR7 deficient mice model was constructed on the basis of Gene Knockout Technique in normal fed mice. (7) Model+TLR7 deficient group: TLR7 deficient model was constructed by gene knockout in modeling mice.

Behavioral standards for modeling: in the Normal group, there were only slight scratching, sneezing or coughing during the process. Mice in the Model group had symptoms of irritability, scratching ears and gills, sneezing or choking, shortness of breath and evident abdominal contraction. Besides, with the prolonged duration of stimulation, the former symptoms became more serious, such as hair color change and tarnish, slow reaction, fecal incontinence, head and face pruritus, forelimb retraction, shortness of breath, back upright with arched back and other symptoms, which indicated a successful modeling was successful. All animal experiments in this study were in accordance with the experimental animal management and use principles locally with the Approval of the Ethics Committee.

Bronchoalveolar Lavage and Lavage Fluid Treatment, Retention and Treatment of Bronchus and Lung Tissues

The mice were anesthetized with 1% phenobarbital sodium, followed by the removal of eyeballs and animal sacrifice. After disinfection with 75% ethanol, the skin was cut, and the subcutaneous tissue and muscle were separated passively. After the trachea was fully exposed, a 22 G venous indwelling needle was used for endotracheal intubation. After the needle entered about 0.5 cm, the needle core was pulled out, and the surgical suture was inserted under the trachea to fix the indwelling needle. Following lavage twice with 0.5 ml of pre-cooled sterilized phosphate-buffered saline (PBS), the chest of mice was gently squeezed while the bronchoalveolar lavage fluid (BALF) was sucked back slowly. If the recovery rate was >80%, it was regarded as qualified. There was no significant difference in the recovery quantity of BALF among groups. After alveolar lavage, the fluid was centrifuged for 5 min (1000 r/min), and the supernatant was frozen at - 80°C for further usage.

With the collection of frozen BALF and re-suspension, 10 μL of the BALF was placed on the Cell Counting Chamber to count the total number of cells. The remaining BALF was centrifuged at 4°C, and the cell precipitate was resuspended with proper amount of PBS. Then, 100 μL cell suspension was taken for sample loading after mixing, followed by centrifugal separation using WESCOR. After natural drying, cell slides were fixed with 95% ethanol. After drying, cells were stained with Diff-Quik. The total number of BALF cells, eosinophils, neutrophils, lymphocytes and monocyte macrophages were observed, with 400 nucleated cells counted under the microscope. After alveolar lavage, the left lung of mice was fixed with 4% paraformaldehyde for 24 h, then embedded in paraffin, fixed and sliced eventually.

Hematoxylin-eosin (HE) Staining

The left lung tissue preserved in 4% paraformaldehyde was fixed for 24 h, and then dehydrated by gradient ethanol, which was 70% ethanol for 1 h, 80% ethanol for 1 h, 95% ethanol for 1 h, 95% ethanol for 1 h and 95% ethanol for 1 h, followed by anhydrous ethanol for 1 h, transparent processing with xylene, embedded in paraffin and sliced of 5 μm in thickness. As for HE staining, xylene was used for dewaxing twice, 10 min each time, followed by gradient ethanol hydration (anhydrous ethanol for 1min, 95% ethanol for 1 min, 80% ethanol for 1 min, and 70% ethanol for 1 min); hematoxylin staining; soaking in HCI+ ethanol for seconds; Eosin staining; gradient ethanol hydration (95% ethanol for 1 min, 95% ethanol for 1 min, and anhydrous ethanol for 1 min), transparent processing with xylene; and sealing with neutral resin after drying. The morphological structure of lung tissue, the injury of airway epithelium, the pathological changes around airway and the infiltration of inflammatory cells were observed under light microscope.

Immunohistochemical Detection

Frozen tissue sections were placed in a wet box and washed with PBS solution for 3 times (2 min each). The PBS solution was removed and the fluid around the tissue section was dried. A 3% hydrogen peroxide solution was dropped in the sections, which were then incubated for 10 min to block endogenous peroxidase. After PBS solution washing for 3 times (2 min each), antigen repair was performed with the use of microwave citric acid buffer (250 mL), high-temperature treatment for 6 min, low-fire treatment in the microwave oven for 15 min, and cooling at room temperature for 20 min. With repeated PBS washing three times (2 min each), the primary antibodies of TLR7, IKKα and NF-κBp65 were added and incubated overnight. After PBS washing, and tissue section drying, the secondary antibody (goat-anti-rabbit IgG-HRP) was added and incubated at room temperature for 20 min. Following similar steps of PBS washing as above, DAB solution was prepared immediately and used to develop. The color of development was controlled under microscope. After that, tissue sections received hematoxylin re-staining for 30 s, differentiation by HCI+ ethanol, washing with distilled water and re-staining again. Sealing was realized by using neutral resin following gradient ethanol hydration (70%-80%-90%-95%-anhydrous ethanol) and transparent processing with xylene. The experiment was performed to count the number of TLR7, IKKα and NF-κBp65 positive cells, and the percentage of positive cells in the total number of cells was calculated.

Enzyme-linked Immunosorbent Assay (ELISA) Detection

The supernatant of BALF was collected and detected for interleukin (IL)-4, IL-10, IL-12 and IFN-γ according to the instructions of ELISA kit. All kits were purchased from Abcam, Cambridge, UK. The operation steps referred to the manual of the kit. The simple steps were as follows: the ELISA plate was coated with anti-IL-4, IL-10, IL-12 and IFN-γ monoclonal antibodies, placed overnight at 4°C, washed with PBS containing 0.5 mL Tween-20, added with PBS solution containing 10 g/L BSA, and standing for 1h at room temperature. After washing, human IL-4, IL-10, IL-12 and IFN-γ standards at different dilutions and cell culture supernatant were added into each well and kept at room temperature for 2 h. After washing, biotin labeled mouse anti-human IL-4, IL-10, IL-12 and IFN-γ monoclonal antibodies and affinity labeled horseradish peroxidase (HRP) were added, which were left for 1 h at room temperature. After washing, TMB chromogenic agent was added, and the reaction was stopped by adding 100 μL 2 moL/L sulfuric acid. The secretion of IL-4, IL-10, IL-12 and IFN-γ in the culture supernatant was detected by Microplate Reader.

Isolation, Culture and Identification of ASMCS

The mice were killed under abdominal anesthesia by using ketamine and droperidol mixed (0.1 ml/20 g) at the ratio of 1:1, and all the main trachea were obtained aseptically. Under the condition of ice bath, the tracheal tissue was washed in serum-free Dulbecco's Modified Eagle's Medium (DMEM) medium, the cartilage surface was cut off, the tracheal mucosa and submucosa were scraped off with cotton swab, and the cartilage on both sides was separated. After that, the isolated tracheal smooth muscle strips were cut into tissue blocks of about 1 mm × 1 mm × 1 mm in size. At 37°C, 0.1% trypsin-0.02% EDTA was used for digestion for 10 min at first, then the 0.1% collagenase digestion solution was changed twice, with digestion for 40 min and 50 min respectively under the same conditions. After washing, stabilizing, blowing, filtering and centrifuging, DMEM medium containing 10% fetal

bovine serum was added. The number of cells was adjusted to 0.5×10^7/L, and then inoculated in 24-well plates with 1 mL per well. The culture flask was then placed in a CO_2 incubator at 37°C for 3 h for drying. The culture flask was turned gently so that the culture medium was just above the surface of the tissue block. After three days of culture in semi-open absolute standing mode, the culture medium was added to 5 ml, and the liquid was completely changed on the sixth day, and then the medium was changed once every three days. After 7 days, the cells were sub-cultured, and the 4th to 6th passage cells were selected for subsequent experiments.

Cell Grouping and Transfection

The third passage cells were digested by trypsin and inoculated into 24-well plates to the monolayer status of growth. Cells were divided into 7 groups according to the design requirements: Control group (ASMCS of the Normal group), pcDNA-TLR7 NC group (ASMCS of the Model group with the transfection of pcDNA-TLR7 NC sequence), siRNA-TLR7 NC group (ASMCS of the Model group with the transfection of siRNA-TLR7 NC sequence), pcDNA-TLR7 group (ASMCS of the Model group with the transfection of pcDNA-TLR7 sequence), siRNA-TLR7 group (ASMCS of the Model group with the transfection of siRNA-TLR7 sequence), Asatone group (ASMCS of the Model group with signaling pathway agonist Asatone treatment), Triptolide group (ASMCS of the Model group with signaling pathway inhibitor Triptolide treatment), and pcDNA-TLR7 +Asatone group (ASMCS of the Model group without the transfection of pcDNA-TLR7 sequence and signaling pathway agonist Asatone treatment). The transfection sequence was constructed by Sangon Biotech (Shanghai) Co., Ltd. Liposome transient transfection was carried out according to the protocol of lipofectamine 2000. The following experiments were carried out after 24-48 h of culture.

Real-time Polymerase Chain Reaction (RT-PCR) Detection

Total RNA was extracted from lung tissue and ASMCs after transfection by using TRIzol (Invitrogen, Carlsbad, CA, USA). The absorbance ratio of RNA samples at 260/280 m wavelength was 1.9-2.0 with Ultraviolet Spectrophotometer. SYBR Primescrip™ RT-PCR kit (TaKaRa, Dalian, China) was used for detection using ABI Prism 7500 (Applied Biosystems, Foster City, CA, USA), and the operation was carried out according to the instructions of the kit. The reaction lasted for 40 cycles at 95°C for 5 s and 60°C for 30 s. Three parallel tubes were made for each sample to be tested and the relative standard substance of each gradient concentration. The amplification dynamic curve and melting curve were automatically drawn by the fluorescence quantitative analysis software. The purity of real-time fluorescent quantitative reaction products was analyzed by melting curve to determine the specificity of the experiment. After PCR reaction, the data were analyzed by 7500 system SDS software, and the relative initial copy number of each sample was calculated. β-actin (F: 5'-CCAGAGCAAGAGAGGCATCC-3', R: 5'-CCGTGGTGGTGAAGCTGTAG-3') was used as the internal reference in the detection of the mRNA level of TLR7 (F: 5'-CCACCAGACCTCTTGATT-3', R: 5'-CCAGATGGTTCAGCCTAC-3') and IDO (F: 5'-GATGAAGAAGTGGGCTTTGC-3', R: 5'-TCCAGTTTGCCAAGACACAG-3'), and the relative transcription level of target mRNA was calculated by relative quantitative method ($2^{-\Delta\Delta CT}$ method). The test was repeated 3 times.

Western Blot Detection

RPA strong lysate (10 times its volume) was used to decompose and homogenize tissues on ice. The supernatant was separated from the homogenate at a low temperature of 17,000 g. the protein content of the sample was determined by bicinchoninic acid assay (BCA) protein content determination kit. The sample buffer was added to the sample protein in the ratio of 1: 4. The protein was completely denatured by boiling in boiling water for 5 min. The supernatant was centrifuged at 17,000 g for 15 min to collect the supernatant. The samples were taken for 7.5% polyacrylamide gel electrophoresis in discontinuous buffer system. Then, the gel was separated, and the protein was transferred to the nitrocellulose membrane. The membrane was sealed with 15% skimmed milk powder (dissolved by TBST) at room temperature. The first antibody [TLR7 (ab124928, dilution ratio of 1:1000), p-IKKα (ab32041, dilution ratio of 1:10,000) and NF-κBp65 (ab16502, dilution ratio of 1:2000)] was added to the membrane and reacted overnight at 4°C. The membrane was washed by Tris-Buffered Saline and Tween-20 (TBST). The corresponding secondary antibody of goat anti-rabbit IgG labeled with Horseradish Peroxidase (HRP) was added and incubated at room temperature for 2 h, followed by TBST

washing again. An appropriate amount of liquid A and B in enhanced chemiluminescence (ECL) reagent box were taken and mixed evenly. Clean filter paper was used to absorb the liquid on the membrane, and the mixed solution was evenly dropped into the membrane, followed by film exposure and development. The integrated density value was analyzed and measured by computer image analysis system. GAPDH was the internal reference. Each group was repeated three times. This method was also applicable to cells.

Detection of 3-(4,5-dimethyl-2-thiazolyl)-2,5-diphenyl-2-H-tetrazolium Bromide (MTT)

After digestion of the cells in logarithmic growth phase with trypsin, the cells were resuspended into cell suspension by complete culture medium, and then the cells were counted by Hemocytometer. The experiment was divided into two groups, with 5 wells in each group, and 100 μL cell suspension was added into each well (most of the cells in each well were 2000 cell/well, and the number of cells was the same in each group). In order to detect the OD value of 24 h, 48 h, 72 h, 96 h and 120 h, each group had 5 96-well plates, followed by incubation in 5% CO_2 incubator at 37°C. On the second day 4 h before the end of culture, the original culture medium remained, and 20 μL of 5 mg/ml MTT was added into each well simultaneously. After MTT was added for 4 h, the used culture medium was removed with a pipette gun, and then 100 μL DMSO was added into each well to terminate the reaction. After that, the oscillator was used to oscillate the plate for 5-10 min, and then the OD value was detected at the wavelength of 490 nm using Microplate Reader, followed by statistical mapping.

Flow Cytometry Detection

After transfection, a part of the cells inoculated in the 6-well plate was cultured and digested with trypsin after growing over all the bottom of the culture plate. The cell suspension digested in each group was collected in 5 ml centrifuge tube, and then centrifuged twice at the speed of 1,500 rpm for 5 min each. The supernatant after centrifugation was discarded, cells were washed with PBS twice, washed with binding buffer again, centrifuged at the same speed for 5 min repeatedly, and then the cell precipitates were collected. Then, the cells were resuspended with staining buffer (binding buffer) to make the final density of cell suspension to be 1×10^6 -1×10^7 cell/ml. An amount of 100 uL cell suspension was collected to make the cell count to be about 1×10^5 -1×10^6. The staining was performed by using fluorescein isothiocyanate/propidium iodide (FITC) labeled Annexin-V (5 uL), and then propidium iodide (PI) nucleic acid embedded dye (5 uL). The staining should be kept away from light at room temperature for 10-15 min, and then transferred to the flow cytometry tube for detection.

Statistical Analysis

SPSS 19.0 (SPSS, IBM, Armonk, NY, USA) was used for statistical analysis. Measurement data were expressed by mean ± standard deviation. Comparison between groups was conducted by independent sample *t*-test. The comparison among groups was conducted by one-way analysis of variance (ANOVA), and then the pairwise comparison was conducted by LSD method. The count data were expressed by percentage and analyzed by chi square test. Statistical significance was determined when $p< 0.05$.

Results

Observation of Pathological Changes in Experimental Mice with Bronchial Asthma Under Different Interventions

According to the results of HE staining in Figure 1, the Normal group had smooth airway epithelium, no submucosal inflammatory cell infiltration and cilia shedding, no airway smooth muscle thickening and no inflammatory exudate infiltrating into alveolar cavity. In the Asthma group, the lungs showed homogeneous expansion, white color, irregular dark red blood flushing areas, and white and viscous exudates were detected on the section. Meanwhile, a large number of inflammatory cells infiltrated around the bronchus and blood vessels in the lung. Inflammatory cells and exudates increased, and mucus embolus formed. Furthermore, immunohistochemical test detection of the positive expression of TLR7, IKKα and NF-κBp65 (Figure 2) revealed that TLR7 was positively expressed in the Normal group, while IKKα and NF-κBp65 showed weak positive expression. While in the Asthma group, TLR7 had weak positive expression, whereas IKKα and NF-κBp65 were highly positively expressed, and the positive cells were brown yellow and increased in the proportion significantly. Compared with the Normal group,

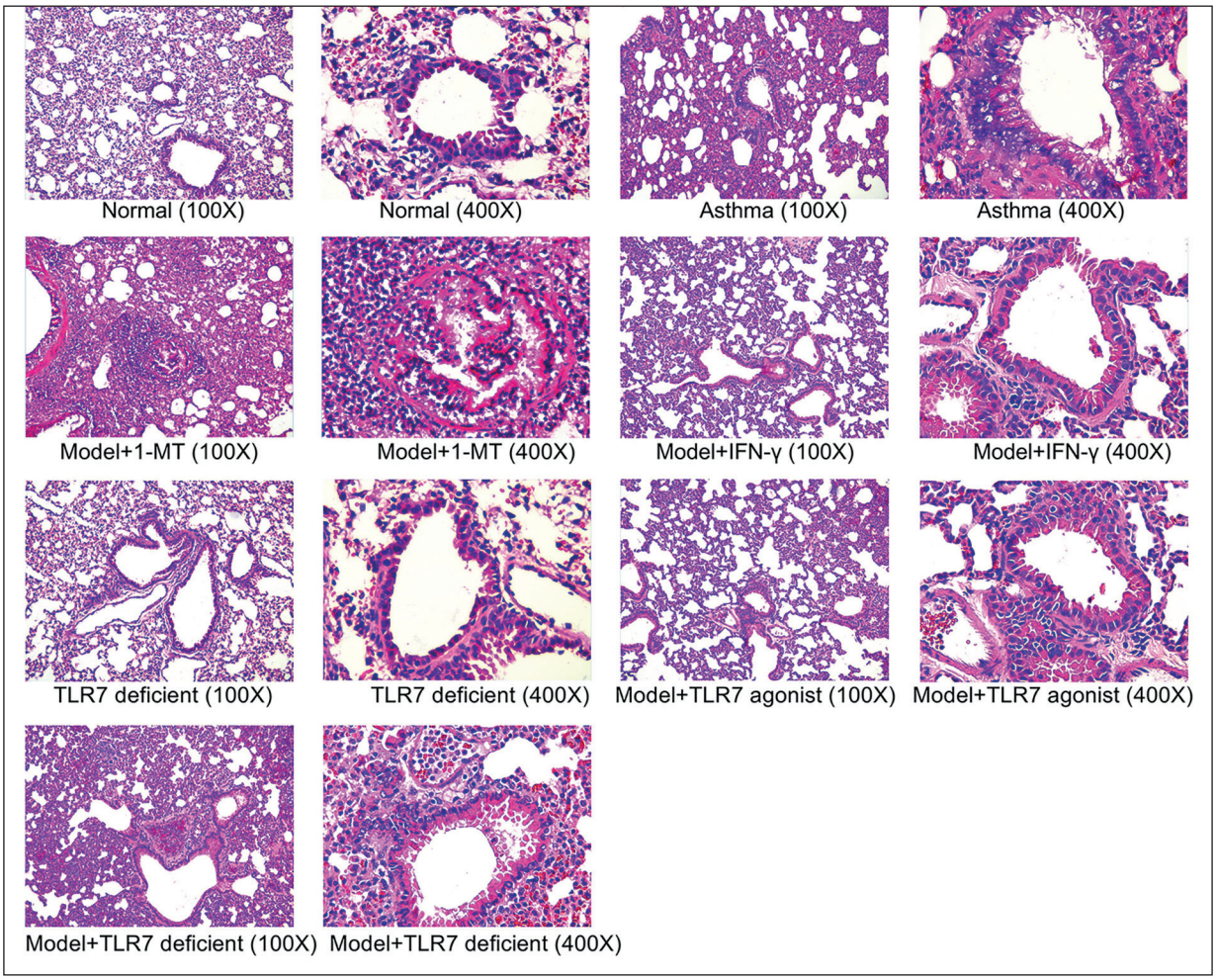

Figure 1. Observation of pathological changes by HE staining in experimental mouse with bronchial asthma under different interventions (100× and 400×).

the positive expression rate of TLR7 in the Asthma group was significantly decreased, and the positive expression rate of IKKα and NF-κBp65 was significantly increased ($p<0.05$). These results suggested pathological deterioration of lung tissue, increased expression of TLR7, and activation of NF-κBp65 signaling pathway after modeling.

Furthermore, Model+1-MT group had a large number of inflammatory cell infiltration, inflammatory cells and exudate increased, while Model+IFN-γ group had decreased inflammatory cell infiltration and exudate. In addition, there was flat airway epithelium with no inflammatory cell infiltration and cilia shedding under the mucosa, no airway smooth muscle thickening and no inflammatory exudate infiltrating into the alveolar cavity in the TLR7 deficient group. Model+TLR7 agonist group was found to have both decreased inflammatory cell infiltration and exudate; while Model+TLR7 deficient group revealed a large number of inflammatory cells infiltration and increased inflammatory cells and exudates.

Observation of Factor Changes Related to Inflammation in Experimental Mice with Bronchial Asthma Under Different Interventions

As listed in Table I in terms of the results of ELISA, the content of IL-4, IL-10, IL-12 and IFN-γ was significantly increased in Asthma group when compared with Normal group ($p<0.05$). These results suggest that there may be increased airway inflammatory response.

Furthermore, there was significantly increase in the content of IL-4, IL-10, IL-12 and IFN-γ in BALF supernatant of the Model+1-MT group

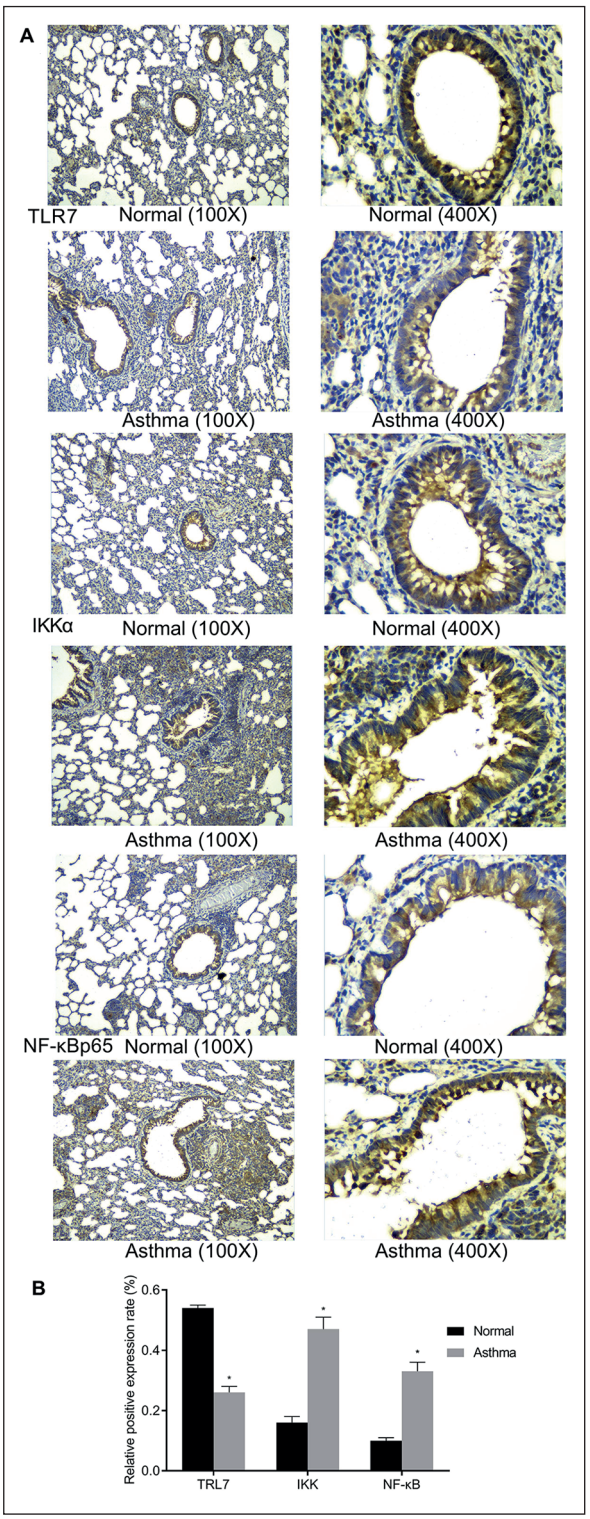

Figure 2. Immunohistochemical analysis of TLR7, IKKα and NF-κBp65 expression in lung tissue of the normal and modeling mice; **A**, Immunohistochemical staining results of TLR7, IKKα and NF-κBp65 expression in lung tissue (100× and 400×); **B**, Statistical analysis of TLR7, IKKα and NF-κBp65; n=10, analysis based on independent sample *t*-test; *Compared with the Normal group, $p<0.05$.

BALF; whereas content of those indexes was markedly decreased ($p< 0.05$). Compared TLR7 deficient group showed no significant change in IL-4, IL-10, IL-12 and IFN-γ in BALF supernatant compared with the Normal group ($p>0.05$), suggesting that TLR7 knockout alone had no significant effect on inflammatory response in mice. Meanwhile, compared with Asthma group, Model+TLR7 deficient group showed significantly increased content of IL-4, IL-10, IL-12 and IFN-γ in BALF supernatant; while Model+TLR7 agonist group had significantly decreased content of IL-4, IL-10, IL-12 and IFN-γ ($p<0.05$).

Observation of Changes in TLR7, IDO and NF-κB Related Factors in Experimental Mice with Bronchial Asthma Under Different Interventions

RT-PCR (Figure 3A) showed that compared with Normal group, Asthma group had decreased mRNA expression levels of TLR7 and IDO ($p< 0.05$). Besides, Western blot detection results (Figure 3B) revealed decreased protein expression of TLR7, as well as increased protein expressions of p-IKKα and NF-κBp65 in Asthma group than those in Normal group ($p<0.05$). Meanwhile, in relative to the Asthma group, Model+1-MT group had evidently decreased mRNA expression levels of TLR7 and IDO, while Model+IFN-γ group indicated remarkably increased mRNA expression levels of TLR7 and IDO ($p<0.05$). At the same time, compared with the Asthma group, Model+1-MT group showed significantly decrease in TLR7 protein expression, increase in the protein expressions of p-IKKα and NF-κBp65; while Model+IFN-γ group had significantly increased protein expression of TLR7, and decrease in the protein expression of p-IKKα and NF-κBp65 ($p<0.05$).

Simultaneously, no significant difference was found between Normal group and TLR7 deficient group ($p>0.05$). Model+TLR7 deficient group had markedly decreased TLR7 and IDO mRNA expression levels, whereas an opposite trend was detected in Model+TLR7 agonist group ($p< 0.05$). Besides, in relative to Asthma group, Model+TLR7 deficient group had significantly decreased protein expression of TLR7, but significantly increased protein expression of p-IKKα and NF-κBp65; while Model+TLR7 agonist group showed an opposite trend of increase in TLR7 but decrease in p-IKKα and NF-κBp65 ($p< 0.05$).

Table I. ELISA detection of inflammatory factors of IL-4, IL-10, IL-12 and IFN-γ in BALF supernatant of mice in the Normal group and Asthma group.

Groups	N	IL-4	IL-10	IL-12	IFN-γ
Normal	10	27.43 ± 4.55	65.34 ± 6.46	43.43 ± 7.00	124.24 ± 16.35
Asthma	10	87.67 ± 12.12*	164.27± 14.38*	99.20 ± 9.75*	265.28 ± 20.12*
Model+1-MT	10	111.24 ± 13.00#	198.29 ± 15.32#	123.28 ± 10.21#	300.24 ± 22.86#
Model+IFN-γ	10	43.76 ± 8.70#	99.21 ± 11.21#	60.20 ± 8.62#	197.34 ± 13.15#
TLR7 deficient	10	26.40 ± 4.15	63.75 ± 6.76	45.26 ± 6.88	121.76 ± 16.48
Model+TLR7 agonist	10	37.84 ± 5.00#	70.26 ± 5.71#	49.50 ± 4.24#	143.02 ± 11.10#
Model+TLR7 deficient	10	120.43 ± 12.64#	204.12 ± 16.00#	128.46 ± 11.65#	296.27 ± 19.99#

Note: n=10, analysis based on one-way analysis of variance; *Compared with the Normal group, $p< 0.05$; #Compared with Asthma group, $p< 0.05$.

Upregulation of TLR7 Gene Expression Inhibited Activation of NF-κB Signaling Pathway in ASMCS Experiment

In accordance with the results of RT-PCR and Western blot analysis (Figure 4), compared with the control group, the expression of TLR7 in other groups with interventions was significantly decreased, and the expression levels of p-IKKα and NF-κBp65 were significantly increased (all $p<0.05$). There was no significant difference in the above indexes between pcDNA-TLR7 NC group and the siRNA-TLR7 NC group (all $p>0.05$). In relative to corresponding NC group of pcDNA-TLR7 NC group and the siRNA-TLR7 NC group, pcDNA-TLR7 group showed increased TLR7 expression while decreased p-IKKα and NF-κBp65, with an opposite trend found in siRNA-TLR7 group (all $p<0.05$). No significant change was found in the expression of TLR7 in both Asatone group and Triptolide group ($p>0.05$), but with significantly increased p-IKKα and NF-κBp65 expression in Asatone group, while decreased p-IKKα and NF-κBp65 expression in Triptolide group (all $p<0.05$). Meanwhile, there was significant increase in TLR7 expression in pcDNA-TRL7+Asatone group ($p<0.05$), yet without significant difference in the expression of p-IKKα and NF-κBp65 ($p>0.05$).

As indicated by the proliferation detection results using MTT test (Figure 5A), compared with the Control, the other groups showed significantly increased proliferation level (all $p<0.05$). Besides, there was no significant difference among pcDNA-TLR7 NC group, siRNA-TLR7 NC group, and pcDNA-TLR7 +Asatone group (all $p>0.05$). Furthermore, pcDNA-TLR7 group and Triptolide group showed decreased proliferation level, while siRNA-TLR7 group and Asatone group showed increased proliferation level (all $p<0.05$). Besides, compared with pcDNA-TLR7 group, pcDNA-TLR7+Asatone group indicated increased proliferation level ($p<0.05$).

In addition, cell apoptosis detection by flow cytometry (Figure 5B,C) showed that compared with Control group, the apoptosis rate showed a significant downward trend in other groups with

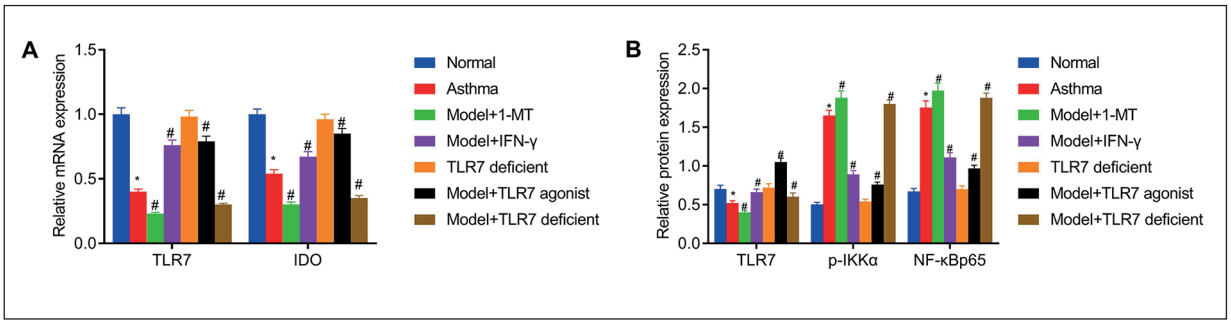

Figure 3. Observation of changes in TLR7, IDO and NF-κB related factors by RT-PCR and Western blot in experimental mice with bronchial asthma under different interventions; **A**, Relative expression detection by using RT-PCR; **B**, Results of Western blot detection in tissues; n=10, analysis based on independent sample *t*-test; *Compared with the Normal group, $p<0.05$; #Compared with the Asthma group, $p<0.05$.

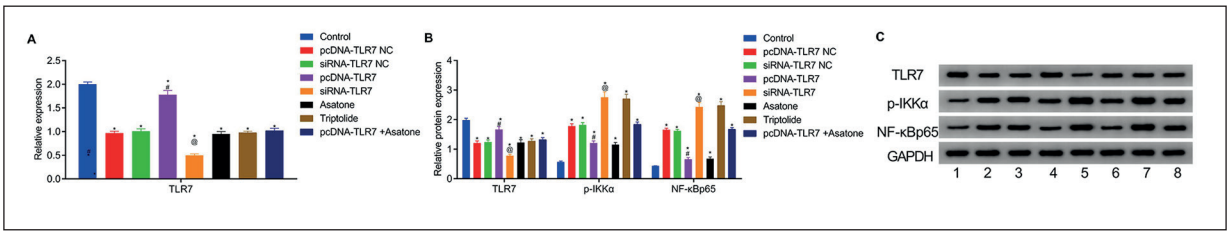

Figure 4. Effect of upregulation of TLR7 gene expression inhibited activation of NF-κB signaling pathway on mRNA and protein expressions in ASMCS experiment. **A**, Results of RT-PCR detection in tissues; **B**, Results of Western blot detection in tissues; The experiment was repeated three times and compared by one-way analysis of variance; **C**, Protein bands by using Western blot; The experiment was repeated three times and compared by one-way ANOVA; *Compared with the Control group, $p<0.05$; #Compared with pcDNA-TLR7 NC group, $p<0.05$; and @Compared with siRNA-TLR7 NC group, $p<0.05$.

interventions, the difference was statistically significant (all $p<0.05$). No significant difference was found in cell apoptosis among pcDNA-TLR7 NC group, siRNA-TLR7 NC group, and pcDNA-TLR7 +Asatone group ($p>0.05$). In addition, pcDNA-TLR7 group and Triptolide group had

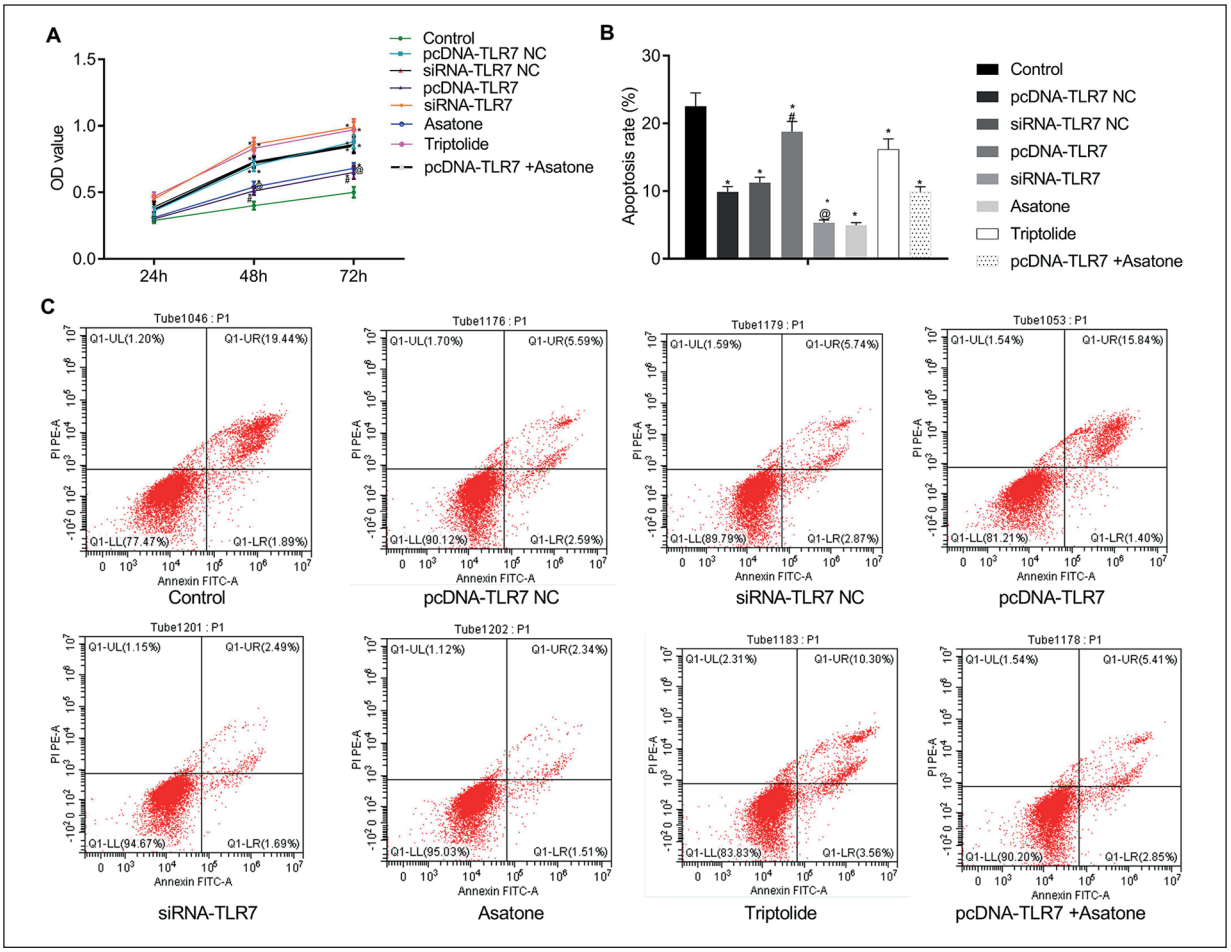

Figure 5. Effect of upregulation of TLR7 gene expression inhibited activation of NF-κB signaling pathway on the proliferation, cell cycle and apoptosis in ASMCS experiment. **A**, Statistical results of cell proliferation by MTT test; The experiment was repeated three times and compared by two-way analysis of variance; **B**, Statistical results of cell apoptosis by flow cytometry; **C**, Experimental results of cell apoptosis by flow cytometry; The experiment was repeated three times and compared by one-way ANOVA; *Compared with the Control group, $p< 0.05$; #Compared with pcDNA-TLR7 NC group, $p<0.05$; and @ Compared with siRNA-TLR7 NC group, $p<0.05$.

significantly increased cell apoptosis rate (all $p<0.05$). Simultaneously, compared with pcDNA-TLR7 group, pcDNA-TLR7 +Asatone group showed decreased apoptosis rate ($p<0.05$).

Discussion

TLR7 belongs to type I transmembrane protein[33], which is mainly composed of extracellular domain, transmembrane domain and intracellular domain. The extracellular domain of TLR7 has leucine-rich repeats, and the intracellular domain has a Toll/IL-1 receptor region, which has high homology with the intracellular domain of IL-1R[34]. It can activate downstream intracellular signaling transduction pathway and realize immune regulation[35]. TLR7 remains in endoplasmic reticulum under resting. When non-cellular components invade cells, TLR7 in endoplasmic reticulum will be transferred to endosome[36]. After recognition and binding with ligands, TLR7 may have changed conformation, can further recruit TIR domain of myeloid differentiation factor 88 (MyD88), activate downstream IRF7 and cause IFN expression[37]. MyD88 can also activate IKK by activating downstream proteins such as IRAK-1/4, TRAF-6, TAK-1 and TAB-1/2. Meanwhile, IKK can phosphorylate IKB, an inhibitor of NF-κB, and then activate NF-κB, and finally promote the expression of various proinflammatory factors (e.g., TNF-α, IL-1, and IL-6) and chemokine IL-8[38,39]. In liver tissue, it has found that IL-12 secreted by plasma cell like dendritic cells (pDCs) after TLR7 activation can drive the immune response of type 1 helper T (Th1) cells, secrete a large amount of IFN-γ, activate phagocytes, antigen-specific cytotoxic T cells, and release various cytokines[40]. However, it is not clear whether TLR7 affects the expression of IFN-γ and induces IDO.

Both IDO and TLR7 play an important role in immune tolerance, but the relationship between them is not very clear. In a mouse model of immune asthma, whether TLR7 can directly induce DCs to produce IDO or whether TLR7 can regulate the expression of IDO through cell signaling transduction is still unknown. Besides, whether its mechanism is related to IKK activation and NF-κB transcription factor regulation needs further study.

At present, inhalation allergen is a more common choice in relative to ovalbumin sensitization, dust mite especially[41]. So far, IDO and TLR7 related to specific immunosuppression have not been reported in the pathogenesis of dust mite sensitized mice. In our study, a mouse model of asthma was induced by intraperitoneal injection of dust mite antigen extract/aluminum hydroxide; meanwhile, ASMCS were isolated from the normal and modeling animals to carry our cell experiments. Our study explored from two parts of animals and cells to verify the role of TLR7 mediated NF-κB signaling pathway on the pathogenesis of bronchial asthma in mice and the intervention effect of IFN-γ.

To be specific, with the successful modeling of asthma, there were decreased positive expressions of TLR7 while increased IKKα and NF-κBp65 positive expressions in the modeling mice, accompanied by significantly increased IL-4, IL-10, IL-12 and IFN-γ levels. It suggested that there might be downregulated expression of TLR7 while activated NF-κB signaling pathway and aggravated inflammatory reaction in asthma modeling mice. With the aim to suppress the progression of asthma and find out potential therapeutic approaches, our experiment further applied 1-MT and IFN-γ, among which 1-MT is an IDO inhibitor to promote inflammatory response, while IFN-γ is an IDO inducer to inhibit inflammatory response. Accordingly, corresponding results revealed a large number of inflammatory cell infiltration, increased IL-4, IL-10, IL-12 and IFN-γ levels, decreased expression levels of TLR7 and IDO, and increased protein expression of p-IKKα and NF-κBp65 after inducing inflammation by using 1-MT. While the inflammation was alleviated and IL-4, IL-10, IL-12 and IFN-γ levels were decreased using IFN-γ. It is suggested that IFN-γ may have a role in suppressing the progression of inflammation in asthma, which may be related to the increased expression of TLR7 while suppressed activation of NF-κB pathway.

In the subsequent experiment, for further identification of the mechanism of action, our study applied the design of gene therapy with the knockout and upregulation of TLR7 gene. Firstly, it was found that knockout of TLR7 gene alone had no significant adverse effect on normal mice, suggesting the feasibility and safety of the proposed approach in our model. Similarly, it was observed that knockout of TLR7 gene in modeling mice showed decreased TLR7 expression, indicating successful knockout, which resulted in aggravated inflammation, increased IL-4, IL-10, IL-12 and IFN-γ levels, and increased protein

expression of p-IKKα and NF-κBp65. While the use of TLR7 agonist in modeling mice revealed the opposite results that the inflammation was relieved and the activation of NF-κB signaling pathway was inhibited. All the above results highlight potential positive role of TLR7 in asthma, which may be associated with the activation of NF-κB signaling pathway.

In this way, our study further carried out cell transfection experiments in the isolated ASMCS, and it was proven that upregulated expression of TLR7 and inhibited activation of NF-κB signaling pathway using Triptolide both resulted in decreased p-IKKα and NF-κBp65, decreased proliferation level, and increased cell apoptosis; while the contrary results were found by suppressing TLR7 expression and activating this pathway using Asatone, yet with no significant difference when upregulating TLR7 combined with Asatone. Significantly, it shall be noted that in relative to treatment by upregulating TLR7 expression, combined treatment of TLR7 upregulation and Asatone reversed the beneficial role of upregulated TLR7 expression and led to increased p-IKKα and NF-κBp65, increased proliferation level, and decreased cell apoptosis. To this end, our study indicated that upregulation of TLR7 expression may exert a positive role in suppressing asthma, which may be related to the inhibited activation of NF-κB pathway. It can help to alleviate inflammation and suppress proliferation, re-distribute cell cycle and increase cell apoptosis.

Conclusions

Collectively, our study for the first time identifies that upregulation of TLR7 can reduce airway inflammation, inhibit ASMCS proliferation and thus promote cell apoptosis in asthmatic mice by suppressing the activation of NF-κB signaling pathway. Meanwhile, the activation of the proposed pathway can reverse the favorable role of upregulated TLR7 expression. Besides, IFN-γ can exert a protective role in suppressing the progression of inflammation in asthma. Our study may provide reference for the treatment of asthma on the basis of genetic intervention from the aspects of animal and cell experiment evidence. Further large-scale animal retest and human experiments will be better to confirm the findings in our study, so as to improve and broaden the therapeutic choices for asthma.

Conflict of Interest

The Authors declare that they have no conflict of interests.

References

1) Weigle WO. Immunologic tolerance: development and disruption. Hosp Pract (Off Ed) 1995; 30: 81-84, 89-92.
2) Sennikov SV, Khantakova JN. Role of T-cell subpopulations in the immunologic tolerance induction. Immunologiya 2017; 38: 239-244.
3) Palomares O, Akdis M, Martín-Fontecha M, Akdis CA. Mechanisms of immune regulation in allergic diseases: the role of regulatory T and B cells. Immunol Rev 2017; 278: 219-236.
4) Abramson J, Husebye ES. Autoimmune regulator and self-tolerance - molecular and clinical aspects. Immunol Rev 2016; 271: 127-140.
5) Veza S, Rodríguez-Perez R, Carretero P, Juste S, Caballero ML. Occupational allergic bronchial asthma induced by Lallzyme EX-V, an enzymatic blend sourced from Aspergillus niger used as additive in the wine industry. Occup Environ Med 2015; 72: 237-238.
6) Huber M, Lohoff M. Change of paradigm: CD8+ T cells as important helper for CD4+ T cells during asthma and autoimmune encephalomyelitis. Allergo J Int 2015; 24: 8-15.
7) Amin K. The Role of the T lymphocytes and Remodeling in Asthma. Inflammation 2016; 39: 1475-1482.
8) Heilmann RM, Suchodolski JS. Is inflammatory bowel disease in dogs and cats associated with a Th1 or Th2 polarization? Vet Immunol Immunopathol 2015; 168: 131-134.
9) Odeh AN, Simecka JW. Regulatory CD4+CD25+ T Cells Dampen Inflammatory Disease in Murine Mycoplasma Pneumonia and Promote IL-17 and IFN-γ Responses. PLoS One 2016; 11: e0155648.
10) Zoso A, Mazza EM, Bicciato S, Mandruzzato S, Bronte V, Serafini P, Inverardi L. Human fibrocytic myeloid-derived suppressor cells express IDO and promote tolerance via Treg-cell expansion. Eur J Immunol 2014; 44: 3307-3319.
11) Holmgaard RB, Zamarin D, Li Y, Gasmi B, Munn DH, Allison JP, Merghoub T, Wolchok JD. Tumor-Expressed IDO Recruits and Activates MDSCs in a Treg-Dependent Manner. Cell Rep 2015; 13: 412-424.
12) Banzola I, Mengus C, Wyler S, Hudolin T, Manzella G, Chiarugi A, Boldorini R, Sais G, Schmidli TS, Chiffi G, Bachmann A, Sulser T, Spagnoli GC, Provenzano M. Expression of Indoleamine 2,3-Dioxygenase Induced by IFN-γ and TNF-α as Potential Biomarker of Prostate Cancer Progression. Front Immunol 2018; 9: 1051.
13) Wang X, Zhang Q, Qiu Y, Xie W, Zhang K, Jiang G. Sodium butyrate down-regulates IFN-γ-

induced indoleamine 2, 3 dioxygenase and promotes its acetylation and ubiquitination in CNE2 nasopharyngeal carcinoma cells. Xi Bao Yu Fen Zi Mian Yi Xue Za Zhi 2015; 31: 487-490.

14) Li Q, Harden JL, Anderson CD, Egilmez NK. Tolerogenic Phenotype of IFN-γ-Induced IDO+ Dendritic Cells Is Maintained via an Autocrine IDO-Kynurenine/AhR-IDO Loop. J Immunol 2016; 197: 962-970.

15) Xiang N, He M, Ishaq M, Gao Y, Song F, Guo L, Ma L, Sun G, Liu D, Guo D, Chen Y. The DEAD-Box RNA Helicase DDX3 Interacts with NF-κB Subunit p65 and Suppresses p65-Mediated Transcription. PLoS One 2016; 11: e0164471.

16) Maehara K, Hasegawa T, Isobe KI. A NF-kappaB p65 subunit is indispensable for activating manganese superoxide: dismutase gene transcription mediated by tumor necrosis factor-alpha. J Cell Biochem 2000; 77: 474-486.

17) Huang N, Liu K, Liu J, Gao X, Zeng Z, Zhang Y, Chen J. Interleukin-37 alleviates airway inflammation and remodeling in asthma via inhibiting the activation of NF-κB and STAT3 signalings. Int Immunopharmacol 2018; 55:198-204.

18) Huang W, Li ML, Xia MY, Shao JY. Fisetin-treatment alleviates airway inflammation through inhibition of MyD88/NF-κB signaling pathway. Int J Mol Med 2018; 42: 208-218.

19) Huang CQ, Li W, Wu B, Chen WM, Chen LH, Mo GW, Zhang QF, Gong L, Li J, Zhang HC, Zhu HM, Zeng QZ. Pheretima aspergillum decoction suppresses inflammation and relieves asthma in a mouse model of bronchial asthma by NF-κB inhibition. J Ethnopharmacol 2016; 189: 22-30.

20) Xu W, Yang G, Duan J, Wang Y, Yao W, Liu X, Chen X, Ding Y, Wang Y, He J. Effects of Toll-like receptors on indoleamine 2, 3-dioxygenase mRNA levels in human trophoblast HTR-8/SVneo cells]. Nan Fang Yi Ke Da Xue Xue Bao 2013; 33: 1559-1564.

21) Wang D, Jiang W, Lakshmi B, DiMuzio J, Zhu F, Agrawal S. Creating the tumor microenvironment for effective immunotherapy: Antitumor activity of intratumoral IMO-2125, a TLR9 agonist is further enhanced by inhibition of indoleamine-pyrrole 2,3-dioxygenase (IDO). Exp Mol Ther 2016; 76: 3847.

22) Agaugué S, Perrin-Cocon L, Coutant F, André P, Lotteau V. 1-Methyl-tryptophan can interfere with TLR signaling in dendritic cells independently of IDO activity. J Immunol 2006; 177: 2061-2071.

23) Al-Anazi MR, Matou-Nasri S, Abdo AA, Sanai FM, Alkahtani S, Alarifi S, Alkahtane AA, Al-Yahya H, Ali D, Alessia MS, Alshahrani B, Al-Ahdal MN, Al-Qahtani AA. Association of Toll-Like Receptor 3 Single-Nucleotide Polymorphisms and Hepatitis C Virus Infection. J Immunol Res 2017; 2017: 1590653.

24) Sophia I, Sejian V, Bagath M, Raghavendra B. Quantitative expression of hepatic toll-like receptors 1–10 mRNA in Osmanabadi goats during different climatic stresses. Small Ruminant Res 2016; 141: 11-16.

25) Oh GS, Kim HJ, Choi JH, Shen A, Kim CH, Kim SJ, Shin SR, Hong SH, Kim Y, Park C, Lee SJ, Akira S, Park R, So HS. Activation of lipopolysaccharide-TLR4 signaling accelerates the ototoxic potential of cisplatin in mice. J Immunol 2011; 186: 1140-1150.

26) Voron'ko OE, Dmitrieva-Zdorova EV, Latysheva EA, Aksenova MG, Storozhakov GI, Bodoev NV, Archakov AI. CARD15 and TLR4 genes polymorphisms in atopic bronchial asthma]. Mol Biol (Mosk) 2011; 45: 831-839.

27) Hussein YM, Awad HA, Shalaby SM, Ali AS, Alzahrani SS. Toll-like receptor 2 and Toll-like receptor 4 polymorphisms and susceptibility to asthma and allergic rhinitis: a case-control analysis. Cell Immunol 2012; 274: 34-38.

28) Törmänen S, Korppi M, Teräsjärvi J, Vuononvirta J, Koponen P, Helminen M, He Q, Nuolivirta K. Polymorphism in the gene encoding toll-like receptor 10 may be associated with asthma after bronchiolitis. Sci Rep 2017; 7: 2956.

29) Kandimalla ER, Bhagat L, Wang D, Yu D, Sullivan T, La Monica N, Agrawal S. Design, synthesis and biological evaluation of novel antagonist compounds of Toll-like receptors 7, 8 and 9. Nucleic Acids Res 2013; 41: 3947-3961.

30) Kanno A, Tanimura N, Ishizaki M, Ohko K, Motoi Y, Onji M, Fukui R, Shimozato T, Yamamoto K, Shibata T, Sano S, Sugahara-Tobinai A, Takai T, Ohto U, Shimizu T, Saitoh S, Miyake K. Targeting cell surface TLR7 for therapeutic intervention in autoimmune diseases. Nat Commun 2015; 6: 6119.

31) Moisan J, Camateros P, Thuraisingam T, Marion D, Koohsari H, Martin P, Boghdady ML, Ding A, Gaestel M, Guiot MC, Martin JG, Radzioch D. TLR7 ligand prevents allergen-induced airway hyperresponsiveness and eosinophilia in allergic asthma by a MYD88-dependent and MK2-independent pathway. Am J Physiol Lung Cell Mol Physiol 2006; 290: L987-L995.

32) Dai J, Yin KS, Sun PL. Effects of imiquimod on airway hyperresponsiveness and airway remodeling in an asthmatic mouse model Acta Universitatis. Medicinalis Nanjing 2009; 29: 50-54.

33) Luo Z, Su R, Wang W, Liang Y, Zeng X, Shereen MA, Bashir N, Zhang Q, Zhao L, Wu K, Liu Y, Wu J. EV71 infection induces neurodegeneration via activating TLR7 signaling and IL-6 production. PLoS Pathog 2019; 15: e1008142.

34) Kawamoto T, Ii M, Kitazaki T, Iizawa Y, Kimura H. TAK-242 selectively suppresses Toll-like receptor 4-signaling mediated by the intracellular domain. Eur J Pharmacol 2008; 584: 40-48.

35) Bao M, Liu YJ. Regulation of TLR7/9 signaling in plasmacytoid dendritic cells. Protein Cell 2013; 4: 40-52.

36) Petes C, Odoardi N, Gee K. The Toll for Trafficking: Toll-Like Receptor 7 Delivery to the Endosome. Front Immunol 2017; 8: 1075.

37) Kitagawa Y, Sakai M, Funayama M, Itoh M, Gotoh B. Human Metapneumovirus M2-2 Protein Acts as a Negative Regulator of Alpha Interferon Production by Plasmacytoid Dendritic Cells. J Virol 2017; 91: e00579-17.

38) Lee EK, Chung KW, Kim YR, Ha S, Kim SD, Kim DH, Jung KJ, Lee B, Im E, Yu BP, Chung HY. Small RNAs induce the activation of the pro-inflammatory TLR7 signaling pathway in aged rat kidney. Aging Cell 2017; 16: 1026-1034.

39) Dovedi SJ, Melis MH, Wilkinson RW, Adlard AL, Stratford IJ, Honeychurch J, Illidge TM. Systemic delivery of a TLR7 agonist in combination with radiation primes durable antitumor immune responses in mouse models of lymphoma. Blood 2013; 121: 251-259.

40) Rubtsova K, Rubtsov AV, Halemano K, Li SX, Kappler JW, Santiago ML, Marrack P. T Cell Production of IFNγ in Response to TLR7/IL-12 Stimulates Optimal B Cell Responses to Viruses. PLoS One 2016; 11: e0166322.

41) Singh VP, Mabalirajan U, Pratap K, Bahal D, Maheswari D, Gheware A, Bajaj A, Panda L, Jaiswal A, Ram A, Agrawal A. House dust mite allergen causes certain features of steroid resistant asthma in high fat fed obese mice. Int Immunopharmacol 2018; 55: 20-27.